Activation of Mammalian Target of Rapamycin Signaling Pathway Contributes to Tumor Cell Survival in Anaplastic Lymphoma Kinase–Positive Anaplastic Large Cell Lymphoma

Francisco Vega,[1] L. Jeffrey Medeiros,[1] Vasiliki Leventaki,[1] Coralyn Atwell,[1] Jeong Hee Cho-Vega,[2] Ling Tian,[3] Francois-Xavier Claret,[3] and George Z. Rassidakis[1]

Departments of [1]Hematopathology, [2]Molecular Pathology, and [3]Molecular Therapeutics, The University of Texas M.D. Anderson Cancer Center, Houston, Texas

Abstract

Anaplastic lymphoma kinase (ALK)–positive anaplastic large cell lymphoma (ALCL) frequently carries the t(2;5)(p23;q35) resulting in aberrant expression of chimeric nucleophosmin-ALK. Previously, nucleophosmin-ALK has been shown to activate phosphatidylinositol 3-kinase (PI3K) and its downstream effector, the serine/threonine kinase AKT. In this study, we hypothesized that the mammalian target of rapamycin (mTOR) pathway, which functions downstream of AKT, mediates the oncogenic effects of activated PI3K/AKT in ALK+ ALCL. Here, we provide evidence that mTOR signaling phosphoproteins, including mTOR, eukaryotic initiation factor 4E–binding protein-1, p70S6K, and ribosomal protein S6, are highly phosphorylated in ALK+ ALCL cell lines and tumors. We also show that AKT activation contributes to mTOR phosphorylation, at least in part, as forced expression of constitutively active AKT by myristoylated AKT adenovirus results in increased phosphorylation of mTOR and its downstream effectors. Conversely, inhibition of AKT expression or activity results in decreased mTOR phosphorylation. In addition, pharmacologic inhibition of PI3K/AKT down-regulates the activation of the mTOR signaling pathway. We also show that inhibition of mTOR with rapamycin, as well as silencing *mTOR* gene product expression using mTOR-specific small interfering RNA, decreased phosphorylation of mTOR signaling proteins and induced cell cycle arrest and apoptosis in ALK+ ALCL cells. Cell cycle arrest was associated with modulation of G_1-S-phase regulators, including the cyclin-dependent kinase inhibitors $p21^{waf1}$ and $p27^{kip1}$. Apoptosis following inhibition of mTOR expression or function was associated with down-regulation of antiapoptotic proteins, including c-FLIP, MCL-1, and BCL-2. These findings suggest that the mTOR pathway contributes to nucleophosmin-ALK/PI3K/AKT-mediated tumorigenesis and that inhibition of mTOR represents a potential therapeutic strategy in ALK+ ALCL. (Cancer Res 2006; 66(13): 6589-97)

Introduction

Anaplastic large cell lymphoma (ALCL) is an aggressive form of malignant lymphoma of T/null lineage (1). A subset of ALCL tumors carries chromosomal aberrations involving the anaplastic lymphoma kinase (*alk*) gene on chromosome 2p23 resulting in ALK overexpression (2). The most common of these aberrations is the t(2;5)(p23;q35), which results in expression of the chimeric protein, nucleophosmin-ALK (3). Recent studies have established that nucleophosmin-ALK mediates oncogenesis, at least in part, through phosphorylation/activation of the serine/threonine kinase AKT (4, 5). AKT is a downstream effector of phosphatidylinositol 3-kinase (PI3K) and a critical mediator of mammalian target of rapamycin (mTOR) activity (6). However, the activation status of the mTOR pathway in ALK+ ALCL is unknown. Studying the status of the mTOR pathway in ALK+ ALCL is important because it may provide a rationale for a novel therapeutic strategy for these tumors.

mTOR is a serine/threonine protein kinase that forms two distinct protein complexes within cells: one with the regulatory-associated protein of TOR (raptor) and another with the rapamycin-insensitive companion (rictor; refs. 7, 8). mTOR-raptor complex (composed of mTOR, raptor, and GβL) is sensitive to rapamycin and regulates cell growth, in part, by phosphorylation of the ribosomal protein S6 (rpS6) kinase (p70S6K or S6K1) and subsequent phosphorylation of rpS6 to stimulate protein translation and ribosome biogenesis (9, 10). mTOR-raptor also leads to phosphorylation and inactivation of the eukaryotic initiation factor 4E (eiF4E)–binding protein-1 (4E-BP1), dissociating 4E-BP1 from the RNA cap-binding protein eIF4E, thus promoting cap-dependent translation of mRNA (7, 11, 12). mTOR-rictor complex (composed of mTOR, rictor, and GβL) is not rapamycin sensitive and modulates cell survival and proliferation by direct phosphorylation of AKT on Ser^{473} and by facilitating AKT phosphorylation on Thr^{308} by PDK1 *in vitro* (13).

Rapamycin is a macrolide antibiotic with antitumor activity (14, 15). Recent *in vitro* and *in vivo* studies have shown that rapamycin and its analogues have substantial antitumor activity in hematologic malignancies (16, 17). The mechanism by which rapamycin inhibits mTOR-raptor complex kinase activity is not completely understood. Rapamycin forms an inhibitory complex with the FKBP-rapamycin-binding domain of mTOR, which probably destabilizes the mTOR-raptor interaction and prevents mTOR from phosphorylating p70S6K and 4E-BP1 (18, 19).

In this study, we show that the mTOR pathway is frequently activated in ALK+ ALCL cell lines and tumors and that PI3K/AKT contributes to activation of the mTOR pathway *in vitro*. We also show that inhibition of mTOR expression or activity markedly

Note: Supplementary data for this article are available at Cancer Research Online (http://cancerres.aacrjournals.org/).

Requests for reprints: George Z. Rassidakis, Department of Hematopathology, The University of Texas M.D. Anderson Cancer Center, Unit 54, 1515 Holcombe Boulevard, Houston, TX 77030. Phone: 713-745-2535; Fax: 713-792-7273; E-mail: gzrassidakis@mdanderson.org.

doi:10.1158/0008-5472.CAN-05-3018

decreased activation of the mTOR pathway associated with cell cycle arrest and apoptosis in ALK+ ALCL cells. These findings suggest that activation of mTOR signaling contributes to tumor cell survival in ALK+ ALCL, thus providing a potential therapeutic target in this lymphoma type.

Materials and Methods

Cell lines and reagents. Two ALK+ ALCL cell lines were used, Karpas 299 and SU-DHL1. The cell lines were maintained at 37°C in RPMI 1640 supplemented with 10% FCS in a humidified atmosphere containing 5% CO_2. The PI3K inhibitor, LY294002, the selective AKT inhibitor AKT II, and the mTOR-raptor inhibitor, rapamycin, were purchased from Calbiochem (San Diego, CA). Karpas 299 and SU-DHL1 cells were treated with LY294002 at a concentration of 0, 10, or 20 μg/μL as described elsewhere (5), rapamycin at a concentration of 0, 10, 20, and 40 μg/μL with or without 1 μg/μL doxorubicin, and AKT-II inhibitor (Calbiochem; ref. 20) as indicated. Whole-cell lysates were prepared 24 and 48 hours following treatment.

Immunohistochemistry. Rabbit polyclonal antibodies to total AKT (Santa Cruz Biotechnology, Santa Cruz, CA); mTOR, Ser^{2448}p-mTOR, Ser^{240}/Ser^{244}p-rpS6, Thr^{70}p-4E-BP1, total 4E-BP1, and total eIF4E (Cell Signaling Technology, Beverly, MA); and mouse monoclonal antibodies to Ser^{473}p-AKT and Thr^{389}p-p70S6K (Cell Signaling Technology) were used. ALK expression was assessed using the mouse monoclonal antibody ALK-1 (DakoCytomation, Carpinteria, CA). Immunohistochemical methods were used to assess protein expression in formalin-fixed, paraffin-embedded cell blocks from Karpas 299 and SU-DHL1 and in 31 ALK+ ALCL tumors using methods described previously (21). The diagnosis of ALCL was based on the criteria of the WHO classification (1). Each neoplasm was part of a tissue microarray constructed as described elsewhere (22).

Western blot analysis. Subcellular fractionation was done using the NE-PER nuclear and cytoplasmic extraction kit (Pierce, Rockford, IL) according to the manufacturer's protocol with minor modifications. Western blot analysis was done using standard methods as described previously (21). Rabbit polyclonal antibodies to total AKT (Santa Cruz Biotechnology), rabbit polyclonal antibodies to Ser^{2448}p-mTOR, p70S6K, Ser^{240}/Ser^{244}p-rpS6, Thr^{70}p-4E-BP1, total 4E-BP1, and total eIF4E (Cell Signaling Technology), mouse monoclonal antibodies to Ser^{473}p-AKT and Thr^{389}p-p70S6K (Cell Signaling Technology), and rabbit monoclonal antibodies to rpS6 (Cell Signaling Technology) were used. Mouse monoclonal antibodies were used for p21, MCL-1, BCL-2 (DakoCytomation), p27, cyclin A (BD Biosciences PharMingen, San Diego, CA), BCL-XL (Zymed, South San Francisco, CA), c-FLIP, hemagglutinin (HA; Santa Cruz Biotechnology), and β-actin (Sigma, St. Louis, MO).

Adenovirus infection. Karpas 299 and SU-DHL1 cells were infected with the HA-tagged, constitutively active, adeno-myrAkt adenovirus (23) at a multiplicity of infection (MOI) of 20, shown previously to significantly increase Ser^{473}p-AKT levels in our *in vitro* system (data not shown). Whole-cell lysates were prepared from control and infected cells 48 hours after infection. Expression of adeno-myrAkt in infected cells was confirmed by Western blot analysis using the anti-HA antibody. Infection of Karpas 299 and SU-DHL1 cells with a recombinant adenovirus construct expressing β-Gal (adeno-β-Gal) at the same MOI was used as an additional control in these experiments. Adeno-β-Gal was produced using the Adeno-X TRE-β-Gal virus stock (Clontech, Palo Alto, CA).

Inhibition of mTOR and AKT1 expression with small interfering RNA. The sequences of small interfering RNA (siRNA) targeting the human *mTOR, AKT1*, and *4E-BP1* gene products were purchased from Ambion, Inc. (Austin, TX) and were as follows: *mTOR* sense GGAGUCUACUCGCUUCUAUTT and antisense AUAGAAGCGAGUAGACUCCTC, *AKT1* sense GGGCACUUUCGGCAAGGUGTT and antisense CACCUUGCCGAAAGUGCCCTT, and *4E-BP1* sense GGUACCAGGAUCAUCUAUGTT and antisense CAUAGAUGAUCCUGGUACCTC. The negative control 2 siRNA (Ambion) was also used.

Transient transfections of Karpas 299 and SU-DHL1 cells were done using the Nucleofector solution "T" protocol and appropriate program recommended by Amaxa Biosystems (Gaithersburg, MD) and concentrations of siRNAs as indicated. Cells were harvested at 48 hours following transient transfections with the siRNAs and whole-cell lysates were prepared. Western blot analysis confirmed adequate inhibition of protein expression in transiently transfected cells.

Cell viability and apoptosis studies. Cell viability was evaluated using trypan blue exclusion assay in triplicate. Annexin V staining (BD Biosciences PharMingen) detected by flow cytometry was used to assess apoptosis according to the manufacturer's instructions. Briefly, the cells were washed in ice-cold PBS and resuspended in binding buffer at a concentration of 1×10^6 cells/mL. Subsequently, aliquots of 100 μL (1×10^5 cells/mL) were incubated with 5 μL Annexin V-FITC and 5 μL propidium iodide for 15 minutes in the dark at room temperature and 1×10^4 ungated cells were counted using a flow cytometer (FACSCalibur, Becton Dickinson). All experiments were done in triplicate.

Proliferation assay. Karpas 299 and SU-DHL1 cells were treated with LY294002 or rapamycin in 12-well plates using different concentrations as indicated. At 48 hours, a tetrazolium compound, 3-(4,5-dimethylthiazol-2-yl)-5-(3-carboxymethoxyphenyl)-2-(4-sulfophenyl)-2H-tetrazolium (MTS), was added to each well and MTS-positive cells were counted using the CellTiter 96 AQ_{ueous} cell proliferation assay (Promega, Madison, WI) and μQuant spectrophotometer (Bio-Tek Instruments, Inc., Winooski, VT) according to the manufacturer's instructions.

Bromodeoxyuridine incorporation assay. Cell cycle S-phase fraction was assessed by a colorimetric bromodeoxyuridine incorporation assay. Briefly, 10^4 cells per well were incubated with bromodeoxyuridine diluted 1:100 in 96-well plates for 1 to 1.5 hours at 37°C. An anti-bromodeoxyuridine antibody peroxidase conjugate (Roche Molecular Biochemicals, Mannheim, Germany) was used at a 1:200 dilution according to the manufacturer's recommended protocol. After appropriate washings, the colorimetric reaction was achieved using a substrate (tetramethylbenzidine) and evaluated using a plate reader (μQuant spectrophotometer, Bio-Tek Instruments). Multiple readings were obtained every 5 minutes for 30 minutes to ensure that the colorimetric reaction had reached its end point.

Statistical analysis. χ^2 and Fisher's exact tests were used to compare the expression among the mTOR signaling proteins in ALK+ ALCL tumors. Statistical calculations were done using StatView (Abacus Concepts, Inc., Berkeley, CA).

Results

mTOR pathway is frequently activated in ALK+ ALCL tumors and cell lines. The phosphorylation status of mTOR, 4E-BP1, p70S6K, and rpS6 was immunohistochemically examined in 31 ALK+ ALCL tumors. We also determined the expression of total 4E-BP1 and eIF4E in these tumors. We found that mTOR signaling is frequently activated in ALK+ ALCL (Fig. 1). p-mTOR was detected in 24 of 29 (82.8%) and p-p70S6K (cytoplasmic or nuclear) in 24 of 30 (80%) cases (Table 1). The phosphorylation levels of p-mTOR and p-p70S6K as detected by immunohistochemistry were significantly associated (P = 0.0026, χ^2 test), consistent with previous studies on the causal association of these molecules (24). p-rpS6 was detected in 24 of 31 (77.4%) cases and its phosphorylation level was significantly associated with the phosphorylation level of p-4E-BP1 and total eIF4E (P = 0.016 and 0.029, respectively, χ^2 test). Codetection of all four phosphorylated proteins was seen in 19 of 29 cases (66%; Table 1). Of note, AKT activation in ALK+ ALCL tumors, determined as Ser^{473}p-AKT expression (20), significantly correlated with p-mTOR and p-rpS6 (P = 0.037 and 0.002, respectively, χ^2 test) as well as with total 4E-BP1 and total eIF4E (P = 0.001 and 0.003, respectively, χ^2 test). p-4E-BP1 and total eIF4E were both positive in all 31 ALK+ ALCL tumors examined, but the level of detection was variable. eIF4E was strongly positive in 22 of 31 (71%) tumors.

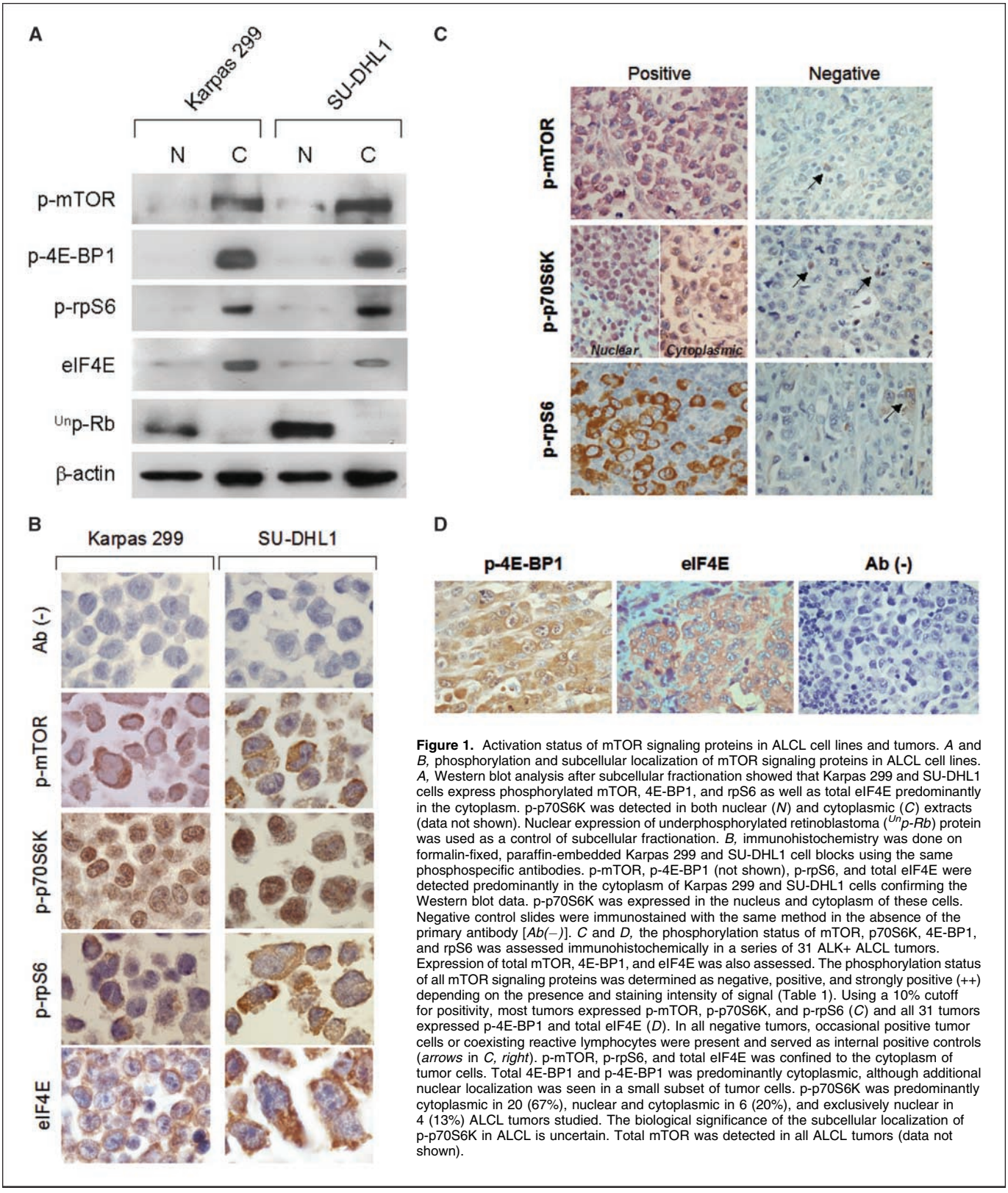

Figure 1. Activation status of mTOR signaling proteins in ALCL cell lines and tumors. *A* and *B,* phosphorylation and subcellular localization of mTOR signaling proteins in ALCL cell lines. *A,* Western blot analysis after subcellular fractionation showed that Karpas 299 and SU-DHL1 cells express phosphorylated mTOR, 4E-BP1, and rpS6 as well as total eIF4E predominantly in the cytoplasm. p-p70S6K was detected in both nuclear (*N*) and cytoplasmic (*C*) extracts (data not shown). Nuclear expression of underphosphorylated retinoblastoma (^{Un}*p-Rb*) protein was used as a control of subcellular fractionation. *B,* immunohistochemistry was done on formalin-fixed, paraffin-embedded Karpas 299 and SU-DHL1 cell blocks using the same phosphospecific antibodies. p-mTOR, p-4E-BP1 (not shown), p-rpS6, and total eIF4E were detected predominantly in the cytoplasm of Karpas 299 and SU-DHL1 cells confirming the Western blot data. p-p70S6K was expressed in the nucleus and cytoplasm of these cells. Negative control slides were immunostained with the same method in the absence of the primary antibody [*Ab(−)*]. *C* and *D,* the phosphorylation status of mTOR, p70S6K, 4E-BP1, and rpS6 was assessed immunohistochemically in a series of 31 ALK+ ALCL tumors. Expression of total mTOR, 4E-BP1, and eIF4E was also assessed. The phosphorylation status of all mTOR signaling proteins was determined as negative, positive, and strongly positive (++) depending on the presence and staining intensity of signal (Table 1). Using a 10% cutoff for positivity, most tumors expressed p-mTOR, p-p70S6K, and p-rpS6 (*C*) and all 31 tumors expressed p-4E-BP1 and total eIF4E (*D*). In all negative tumors, occasional positive tumor cells or coexisting reactive lymphocytes were present and served as internal positive controls (*arrows* in *C, right*). p-mTOR, p-rpS6, and total eIF4E was confined to the cytoplasm of tumor cells. Total 4E-BP1 and p-4E-BP1 was predominantly cytoplasmic, although additional nuclear localization was seen in a small subset of tumor cells. p-p70S6K was predominantly cytoplasmic in 20 (67%), nuclear and cytoplasmic in 6 (20%), and exclusively nuclear in 4 (13%) ALCL tumors studied. The biological significance of the subcellular localization of p-p70S6K in ALCL is uncertain. Total mTOR was detected in all ALCL tumors (data not shown).

We also assessed the baseline activation status of the mTOR pathway in Karpas 299 and SU-DHL1 cell lines. Western blot analysis revealed high levels of p-mTOR associated with high levels of p-p70S6K, p-rpS6, p-4E-BP1, and total eIF4E in both cell lines (Fig. 1).

Inhibition of PI3K/AKT down-regulates mTOR pathway. We assessed the ability of PI3K/AKT to contribute to mTOR pathway activation in Karpas 299 and SU-DHL1 cell lines. Treatment of these cell lines with the PI3K inhibitor, LY294002, resulted in a

Table 1. Expression of mTOR signaling proteins in ALK+ ALCL tumors

	Positive/ total no. (%)	Correlation of expression level (*P*)	
p-mTOR	24/29 (83)	0.026	
p-p70S6K	24/30 (80)*		
p-rpS6P	24/31 (77)		0.029
p-4E-BP1	31/31 (100)	<0.0001	
eIF4E	31/31 (100)†		
p-mTOR/p-4E-BP1/ p-p70S6K/p-rpS6	19/29 (66)		

NOTE: Statistical analysis was based on χ^2 test for all comparisons (3×3 or 2×3 statistical tables), except for the comparison between p-4E-BP1 and eIF4E expression (2×2) where Fisher's exact test was used.

*Predominantly cytoplasmic in 20 (67%), nuclear and cytoplasmic in 6 (20%), and exclusively nuclear in 4 (13%).

†Strong expression was found in 22 of 31 (71%) cases.

concentration-dependent decrease of the phosphorylation levels of AKT, mTOR, 4E-BP1, p70S6K, and S6K (Fig. 2*A* and *B*). These results show that mTOR signaling is regulated, at least in part, by PI3K/AKT and that inhibition of PI3K/AKT decreases the level of activation of mTOR signaling proteins.

Constitutively active AKT results in activation of mTOR pathway. To investigate if AKT activation is sufficient to activate the mTOR pathway in ALK+ ALCL cells, we infected the Karpas 299 and SU-DHL1 cell lines with an adenoviral vector, adeno-myrAkt, expressing constitutively active AKT (23). Constitutive activation of AKT resulted in a substantial increase in the phosphorylation of mTOR, p70S6K, and rpS6 (Fig. 3*A* and *B*).

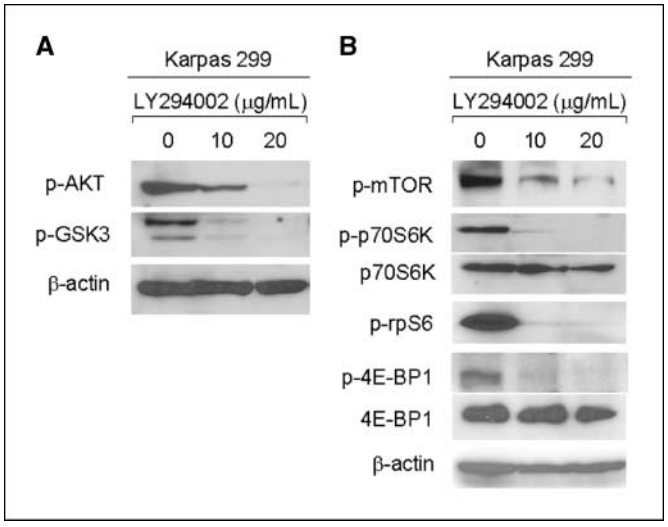

Figure 2. Inhibition of the PI3K/AKT pathway down-regulates mTOR signaling proteins. *A* and *B,* two ALK+ ALCL cell lines, Karpas 299 and SU-DHL1, were treated with the selective PI3K inhibitor, LY294002, at a concentration of 0, 5, 10, or 20 μg/μL. Whole-cell lysates were then prepared at 48 hours. This time point was chosen based on our preliminary results using LY294002 to treat ALCL cells and previously published data (5). Western blot analysis showed high expression levels of all mTOR signaling proteins in both untreated ALCL cell lines. High levels of phosphorylated 4E-BP1, p70S6K, and rpS6 were also detected. After treatment of Karpas 299 and SU-DHL1 cells with increasing concentrations of LY294002, phosphorylation of 4E-BP1, p70S6K, and rpS6 was dramatically decreased. Results for Karpas 299 cells are shown. Similar results were obtained using SU-DHL1 cells.

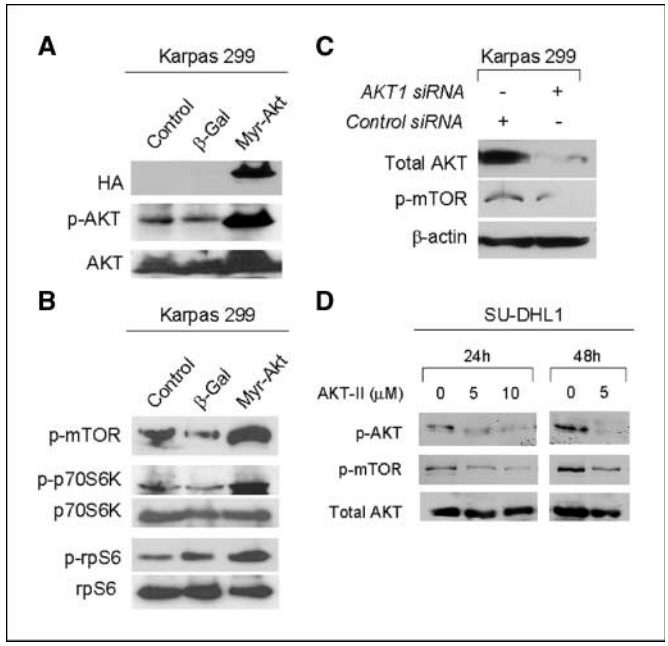

Figure 3. AKT activation contributes to mTOR phosphorylation in ALCL cells. *A* and *B,* adenovirus-mediated overexpression of Ser^{473}p-AKT up-regulates mTOR signaling proteins. Karpas 299 and SU-DHL1 cells were infected with constitutively active, adeno-myrAkt adenovirus (23) at a MOI 20, which results in increased Ser^{473}p-AKT levels. Expression of adeno-myrAkt in infected cells was confirmed by Western blot analysis using a monoclonal antibody specific for the HA tag. An adeno-β-Gal adenovirus construct expressing β-Gal served as a control in this experiment. Whole-cell lysates were prepared from control and infected cells 48 hours after infection. Immunoblots showed strong expression of HA tag in infected ALCL cells but not in control (uninfected or infected with adeno-β-Gal) cells (*A*). Infection of both cell lines with adeno-myrAkt resulted in substantially increased of Ser^{473}p-AKT levels (*A*) associated with increased phosphorylation (activation) of mTOR, p70S6K, and rpS6 (*B*). An increased total eIF4E level was also seen in SU-DHL1 but not Karpas 299 cells following infection with the adeno-myrAkt (not shown). No change in total 4E-BP1 levels was found (not shown). *C* and *D,* inhibition of AKT1 expression or activity decreases mTOR phosphorylation. Karpas 299 and SU-DHL1 cells were transiently transfected with 20 μg AKT1 siRNA or negative control 2 siRNA. Western blot analysis showed almost complete silencing of *AKT1* gene product that was associated with decreased levels of p-mTOR (*C*). Similarly, inhibition of AKT activity using a specific AKT-II inhibitor (20) resulted in decreased p-mTOR levels at a concentration-dependent manner at 24 hours after treatment (*D, left*). At 48 hours, AKT activity was completely inhibited with 5 μmol/L AKT-II inhibitor that was associated with decreased p-mTOR levels (*D, right*).

Inversely, almost complete inhibition of *AKT1* gene expression by AKT1-specific siRNA resulted in decreased p-mTOR levels (Fig. 3*C*). Similarly, inhibition of AKT activity using a specific AKT-II inhibitor (20) resulted in decreased p-mTOR levels (Fig. 3*D*). These results indicate that AKT activation contributes to activation of the mTOR pathway in this *in vitro* system.

Inhibition of mTOR-raptor complex by rapamycin and silencing mTOR by siRNA down-regulates mTOR signaling. Treatment of the Karpas 299 and SU-DHL1 cell lines with increasing concentrations of rapamycin, an inhibitor of the mTOR-raptor complex, resulted in a marked concentration-dependent decrease of the phosphorylation levels of mTOR, p70S6K, 4E-BP1, and total eIF4E (Fig. 4*A*). Of note, treatment of ALCL cell lines with rapamycin also resulted in a slight decrease of Ser^{473} phosphorylation of AKT. Similarly, silencing *mTOR* gene expression by

mTOR-specific siRNA resulted in decreased levels of activation of mTOR signaling proteins and a decrease of p-AKT (Fig. 4*B*).

Inhibition of mTOR induces cell cycle arrest in ALK+ ALCL cells. Previous studies have shown that inhibition of PI3K using LY294002 or wortmannin resulted in decreased cell growth and apoptosis of ALCL cells (5). Here, we also used LY294002 to inhibit the PI3K pathway in Karpas 299 and SU-DHL1 cells. Our findings show that treatment of both cell lines with increasing concentrations of LY294002 led to cell cycle arrest as shown by decreased cell cycle S-phase fraction in a dose-dependent manner (Supplementary Fig. S1A).

As shown in Fig. 5*A*, transient transfection of ALK+ ALCL cells with mTOR siRNA resulted in decreased cell proliferation as assessed by MTS assay. By contrast, no significant changes in cell proliferation were seen following transient transfection with control 4E-BP1 siRNA. Cell cycle studies also showed that

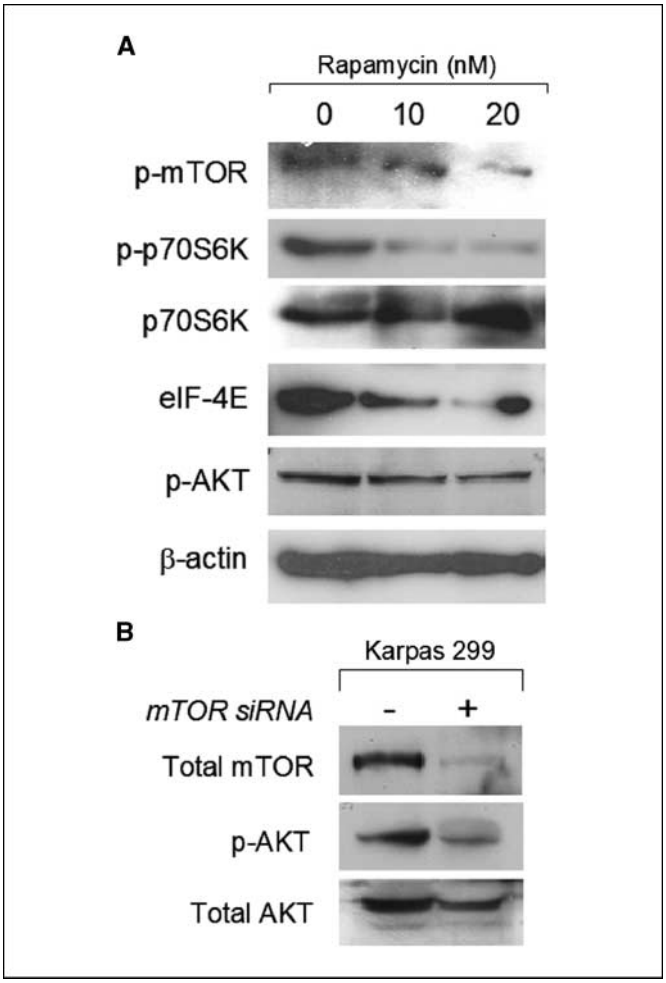

Figure 4. Inhibition of mTOR down-regulates activation of its downstream effectors. mTOR activation and expression in Karpas 299 and SU-DHL1 cells were inhibited using rapamycin and specific mTOR siRNA. ALCL cells were treated with the mTOR inhibitor, rapamycin, at a concentration of 0, 10, 20, or 40 μg/μL (*A*). Results with Karpas 299 cells. Whole-cell lysates were prepared at 48 hours. Immunoblots showed decreased levels of p-mTOR and p-p70S6K after treatment with increasing concentrations of rapamycin. Total eIF4E levels were also decreased. Of note, a slight decrease in p-AKT was also seen following treatment with rapamycin. Transient transfection of ALCL cells with specific mTOR siRNA (20 μg) resulted in almost complete inhibition of mTOR protein expression at 48 hours (*B*) associated with a substantial decrease of p-p70S6K and p-rpS6 (not shown). Notably, a decrease in p-AKT was also found after silencing *mTOR* gene expression (*B*).

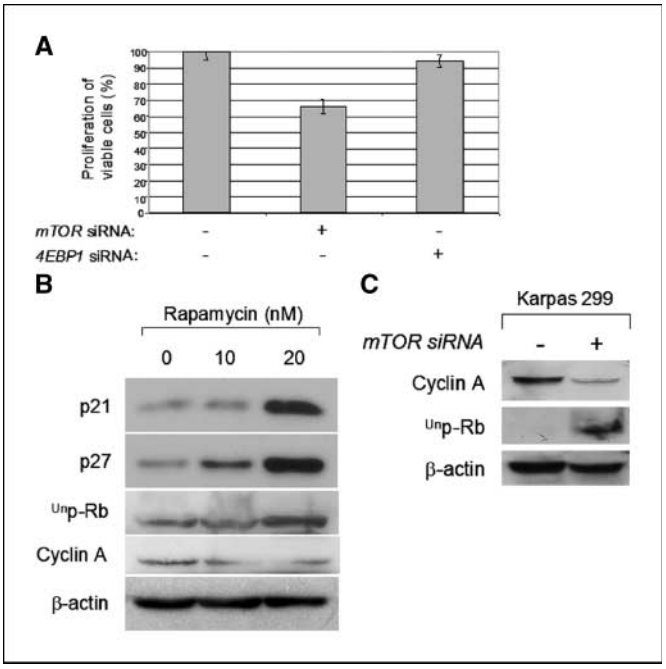

Figure 5. Inhibition of mTOR induces cell cycle arrest in ALCL cells. Karpas 299 and SU-DHL1 cells were transiently transfected with 20 μg mTOR siRNA and whole-cell lysates were prepared at 48 hours. Immunoblots showed almost complete inhibition of mTOR expression (as shown in Fig. 4*B*) that resulted in decreased cell proliferation as assessed by MTS assay (*A*). By contrast, no changes in proliferation of viable cells were observed in control cells transiently transfected with 4E-BP1 siRNA as was expected (*A*). 4E-BP1 is highly phosphorylated and thus inactive in these ALCL cell lines. Western blot analysis following treatment with rapamycin (*B*) or transient transfection with mTOR siRNA (*C*) showed increased levels of the CDK inhibitors $p21^{waf1}$ and $p27^{kip1}$, underphosphorylated retinoblastoma protein, and decreased cyclin A in a dose-dependent manner.

inhibition of mTOR function by using rapamycin or inhibition of mTOR expression by using mTOR-specific siRNA induced cell cycle arrest as shown by a dose-dependent decrease of cell cycle S phase (data not shown).

To evaluate the molecular basis underlying cell cycle arrest after inhibition of mTOR, we assessed several cell cycle regulatory proteins after treatment with rapamycin or specific mTOR siRNA. The cyclin-dependent kinase (CDK) inhibitors $p21^{waf1}$ and $p27^{kip1}$ and underphosphorylated retinoblastoma protein levels were up-regulated and cyclin A levels were decreased in a concentration-dependent manner (Fig. 5*B* and *C*).

These results suggest that inhibition of mTOR-raptor complex or silencing *mTOR* gene expression induced cell cycle arrest at G_1 phase in ALK+ ALCL cells.

Inhibition of mTOR induces apoptosis in ALK+ ALCL cells. As reported previously, inhibition of PI3K resulted in increased apoptosis of ALCL cells (5). Our findings confirm previously published data as treatment of Karpas 299 and SU-DHL1 cells with increasing concentrations of LY294002 led to decreased cell viability and increased apoptosis, as determined by Annexin V staining, in a dose-dependent manner (Supplementary Fig. S1B and C).

To determine if inhibition of mTOR has similar biological effects on ALCL cell lines, we studied cell viability and apoptosis after treatment of Karpas 299 and SU-DHL1 with increasing concentrations of rapamycin and after mTOR-specific siRNA. Both treatments induced a decrease in the number of viable cells. Rapamycin

treatment decreased the number of viable cells in a concentration-dependent manner (Fig. 6*A*). Treatment of Karpas 299 cells with 20 nmol/L rapamycin alone decreased the number of viable cells by approximately one third. Similar results were obtained with SU-DHL1 cells (Supplementary Fig. S2). In addition, we found that treatment with rapamycin sensitized ALK+ ALCL cells to chemotherapy. In our preliminary experiments, using increasing concentrations of doxorubicin, treatment of ALCL cells with 1 μmol/L doxorubicin resulted in no change in cell viability. However, when ALCL cells were treated with 1 μmol/L doxorubicin and increasing concentrations of rapamycin, cell viability was lower compared with treatment with rapamycin alone (data not shown).

Rapamycin treatment also showed a concentration-dependent increase in Annexin V–positive cells, indicating that cell death was secondary to apoptosis (Fig. 6*A*). Morphologic examination of Hoechst-stained cell preparations at 16 hours after treatment with 20 nmol/L rapamycin revealed that Karpas 299 cells showed morphologic evidence of apoptosis, such as nuclear condensation and fragmentation (Fig. 6*A*). Similarly, silencing of *mTOR* also resulted in decreased cell viability and increased Annexin V–positive cells in comparison with control cells and with cells transfected with 4E-BP1-specific siRNA (Fig. 6*B*).

To study the underlying apoptotic mechanisms, expression of apoptosis regulators was assessed after treatment with rapamycin

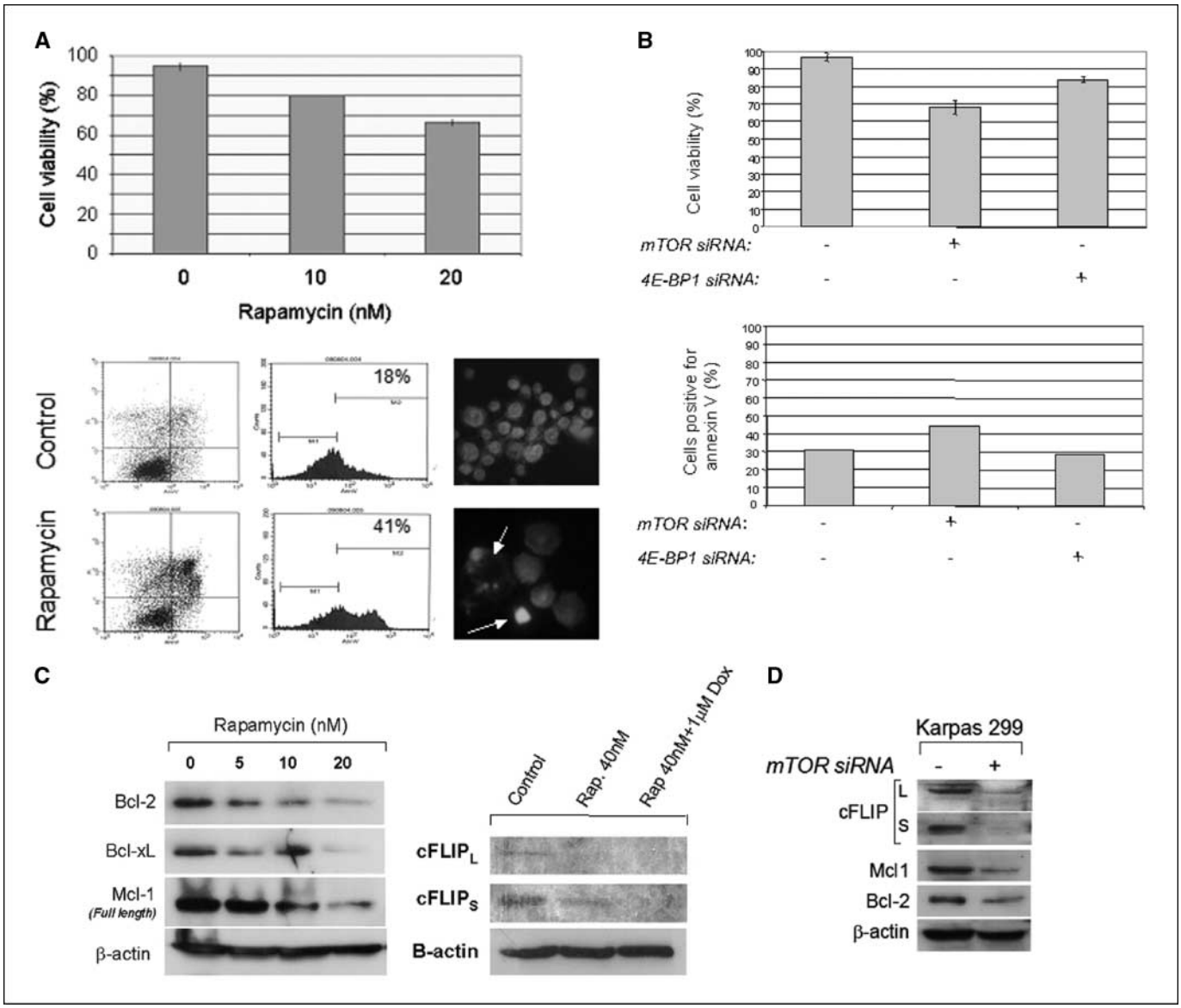

Figure 6. Inhibition of mTOR expression or function induces apoptosis in ALCL cells. Cell viability and apoptosis following treatment of Karpas 299 and SU-DHL1 cells with increasing concentrations of rapamycin and mTOR silencing (siRNA) were assessed using trypan blue exclusion assay and Annexin V staining, respectively. Karpas 299 cell line. Treatment with rapamycin resulted in decreased cell viability in a dose-dependent manner (*A, top*), which was associated with an increase in Annexin V–positive cells. At 48 hours after treatment with 20 μmol/L rapamycin, the percentage of Annexin V–positive cells increased from 18% to 41% (*A, bottom left*). Morphologic examination of the Hoechst-stained cell preparations at 16 hours after treatment with 20 nmol/L rapamycin showed morphologic evidence of apoptosis, such as nuclear condensation and fragmentation in ALCL cells (*A, bottom right*). Transient treatment of ALCL cells with 20 μg mTOR siRNA also resulted in decreased (~30%) cell viability associated with an increase in Annexin V–positive cells in comparison with control and with cells transfected with 4E-BP1-specific siRNA (*B*). Immunoblots showed a concentration-dependent decrease in the antiapoptotic proteins BCL-2, BCL-XL, MCL-1, and c-FLIP (long and short) with increasing concentrations of rapamycin (*C, left*). The decrease in c-FLIP levels was more prominent when rapamycin was combined with 1 μmol/L doxorubicin (*C, right*). Similarly, there was decreased expression of c-FLIP, MCL-1, and BCL-2 after silencing of the *mTOR* gene (*D*).

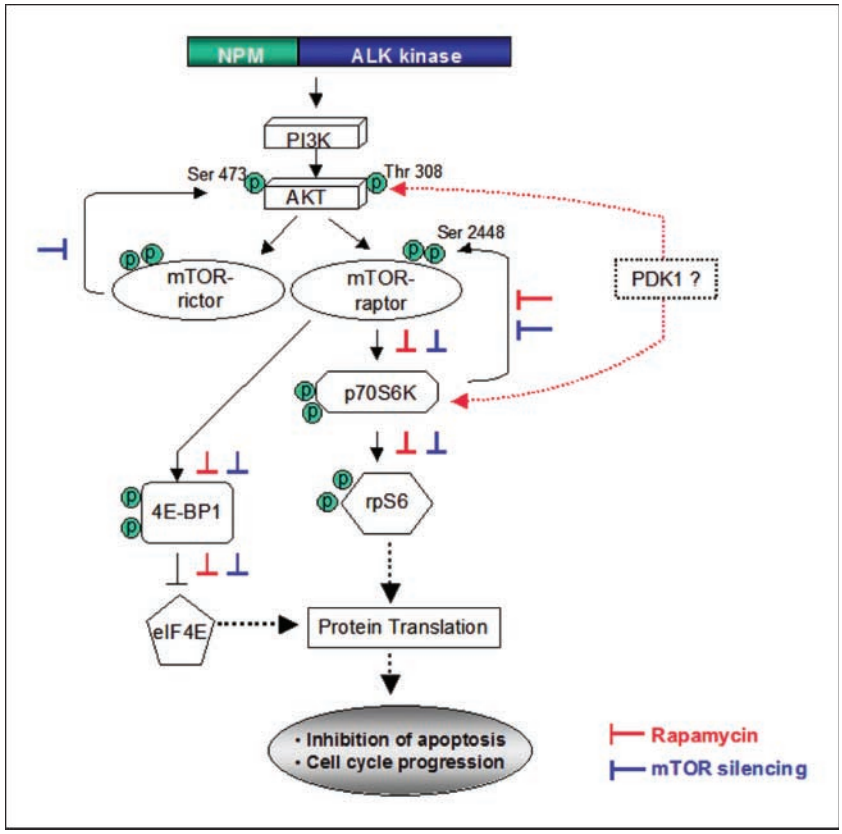

Figure 7. mTOR signaling in ALK+ ALCL oncogenesis. Results from earlier reports and this study support the hypothesis that the PI3K-AKT-mTOR pathway contributes to tumor cell survival in ALCL as shown in this proposed model. In ALK+ ALCL, the most common chromosomal aberration involving the *ALK* locus is the t(2;5)(p23;q35) resulting in expression of the chimeric nucleophosmin-ALK oncoprotein. Nucleophosmin-ALK mediates oncogenesis, at least in part, through phosphorylation/activation of PI3K and its downstream effector, the serine/threonine kinase AKT. Activated AKT, in turn, positively regulates mTOR activity. mTOR can form two distinct complexes, one with raptor and another with rictor. mTOR-raptor complex is sensitive to rapamycin and regulates cell growth, in part, by phosphorylation of p70S6K and subsequently rpS6 and 4E-BP1, thus promoting protein translation. However, the PI3K-AKT-mTOR pathway model seems to be more complex, as recent evidence suggests that rictor-mTOR complex directly phosphorylates AKT on Ser^{473} and facilitates Thr^{308} phosphorylation by PDK1 *in vitro* and mTOR is directly phosphorylated by p70S6K at Ser^{2448}. Taken together, these data suggest that there is a positive feedback loop from p70S6K to mTOR and from mTOR to AKT that possibly accelerates oncogenic signals.

or specific mTOR siRNA. There was a concentration-dependent decrease in the antiapoptotic proteins BCL-2, BCL-XL, c-FLIP (long and short), and full-length MCL-1 with increasing concentrations of rapamycin (Fig. 6*C*). Down-regulation of c-FLIP was even more prominent when rapamycin was combined with 1 μmol/L doxorubicin. Similarly, there was decreased expression of c-FLIP, MCL-1, and BCL-2 after silencing of *mTOR* (Fig. 6*D*).

These findings suggest that inhibition of mTOR induces apoptosis by modulating the expression of proteins involved in both extrinsic and intrinsic (mitochondrial) apoptotic pathways.

Discussion

Emerging data indicate that mTOR is frequently activated in many cancers as a result of genetic alterations of the components in the PI3K/AKT network (25, 26). In ALK+ ALCL, the chimeric protein nucleophosmin-ALK has been shown to activate PI3K and its downstream effector AKT (4). However, the activation status of the mTOR pathway has not been investigated in ALK+ ALCL. This is of interest because effective inhibitors of mTOR are currently available and could form the basis of a novel therapeutic strategy.

Here, we show that the mTOR pathway is activated in ALK+ ALCL. We show that Ser^{2448}p-mTOR (27, 28) is detected at high levels in ALK+ ALCL tumors and cell lines and that the downstream effectors of mTOR, 4E-BP1, p70S6K, and rpS6 are also frequently phosphorylated in ALK+ ALCL.

We also provide evidence that activation of the mTOR pathway in ALK+ ALCL depends, at least in part, on PI3K/AKT. We observed that the phosphorylation level of AKT significantly correlated with the phosphorylation level of mTOR and rpS6 as well as with expression of total 4E-BP1 and eIF4E in ALK+ ALCL tumors. We showed that forced expression of AKT in ALK+ ALCL cell lines resulted in a substantial increase in the phosphorylation of mTOR, p70S6K, and rpS6. We also show that inhibition of the PI3K/AKT pathway in ALK+ ALCL cell lines decreased the level of phosphorylation of mTOR and mTOR signaling proteins. Our findings agree with the generally accepted model of the PI3K/AKT/mTOR pathway in which PI3K/AKT plays an important upstream positive regulatory role in mTOR activation (6, 29).

PI3K/AKT/mTOR is considered to be a central regulatory pathway of protein translation involved in the regulation of cell proliferation, growth, differentiation, and survival (11, 26, 30). Upon activation, mTOR phosphorylates its downstream targets. p70S6K, a key element of mTOR pathway, promotes cell growth by inducing protein synthesis and cell survival by phosphorylating (inactivating) the proapoptotic protein BAD (31, 32). Activated p70S6K, in part through activation of rpS6 (33), increases the translation of 5′-terminal oligopyrimidine tract mRNAs (31, 34). 5′-Terminal oligopyrimidine tract mRNAs exclusively encode components of the translation machinery, including all ribosomal proteins and elongation factors (34). In addition to the cytoplasmic staining for p-p70S6K, we also detected nuclear staining in a significant proportion of ALK+ ALCL tumors. The presence of p70S6K in the nucleus has been reported in other tumor types (35). In addition, others (36) have shown that inhibition of exportin 1, a nuclear export receptor, can lead to accumulation of p70S6K in the nucleus of kidney cells. However, the function of p70S6K in the nucleus is not clear.

The translation initiation factor, eIF4E, is an indirect target of mTOR because it is released by phosphorylation of its repressor 4E-BP1 by mTOR-raptor complex, thereby stimulating cap-dependent translation (7, 11, 12). Although its role in oncogenesis

is poorly understood, expression of eIF4E has been reported in aggressive forms of non-Hodgkin's lymphoma and other cancers (37–39). In agreement with previous studies (39), we observed eIF4E immunoreactivity in all ALCL tumors, with strong expression in almost two thirds of cases. We observed that treatment of ALK+ ALCL cell lines with the PI3K inhibitor, LY294002 (data not shown), and with the mTOR inhibitor, rapamycin, resulted in decreased expression of total eIF4E. It is known that transcription of eIF4E is regulated by MYC and that eIF4E also enhances *MYC* translation (40). It is plausible that a positive stimulatory loop exists wherein eIF4E stimulates *MYC* translation, which in turn stimulates eIF4E transcription, thereby perpetuating positive cell growth signals.

The data presented here are intriguing regarding the AKT/mTOR pathway model. Silencing of total *mTOR* gene expression by siRNA decreased AKT phosphorylation. This finding indicates that mTOR can modulate the activation of AKT and suggests that there is a positive feedback signal to AKT from mTOR (Fig. 7). In agreement with this observation, recently Sarbassov et al. (13) have shown that rictor-mTOR (but not mTOR-raptor) complex directly phosphorylates AKT on Ser^{473} and facilitates Thr^{308} phosphorylation by PDK1 *in vitro*.

Raptor is a 150-kDa mTOR-binding protein that also binds 4E-BP1 and p70S6K (41, 42). Binding of raptor to mTOR is necessary for phosphorylation of 4E-BP1 and p70S6K (Fig. 7). Rapamycin forms an inhibitory complex with the FRB domain of mTOR and inhibits the kinase activities of mTOR protein (18, 19). Our results confirm that rapamycin inhibits activation of the mTOR pathway in ALK+ ALCL cells. Interestingly, we also found that rapamycin decreased the level of Ser^{2448}p-mTOR. Chiang and Abraham (43) have recently shown that mTOR phosphorylation at Ser^{2448} is blocked by rapamycin, and this effect is independent of AKT activation status. Moreover, these authors and others recently have shown that mTOR is directly phosphorylated by p70S6 kinase at Ser^{2448} (43, 44). Because treatment with rapamycin also led to decreased AKT phosphorylation in ALK+ ALCL cells in our *in vitro* study, it is tempting to speculate that an effector protein downstream of mTOR-raptor may contribute directly or indirectly to AKT activation. On theoretical grounds, a good candidate molecule would be p70S6K, because, in aggregate, the recently published findings suggest that there is a positive feedback signal from p70S6K to mTOR (43, 44) and from mTOR to AKT (ref. 13; Fig. 7).

We also show that rapamycin and total mTOR silencing induces cell cycle arrest and apoptosis interfering with proliferation and survival pathways in ALK+ ALCL. Inhibition of mTOR expression or function blocked cell cycle progression from G_1 to S phase associated with modulation of the CDK inhibitors $p21^{waf1}$ and $p27^{kip1}$. Furthermore, we show that induction of apoptosis following inhibition of mTOR signaling involved both the extrinsic (c-FLIP) and the intrinsic (MCL-1 and BCL-2) apoptotic pathways. Similar effects of rapamycin have been shown in other tumor types. It has been shown that mTOR inhibition by rapamycin arrests cells in G_1 phase of the cell cycle and there is evidence that this inhibitory effect occurs via the inhibition of activation of p70S6K1 and 4E-BP1 (45). In addition, inhibition of mTOR activity by rapamycin induces apoptosis (46). Silencing *mTOR* expression using siRNA has not been studied previously in hematopoietic malignancies. Several rapamycin derivatives are currently being assessed in the treatment of patients with advanced cancers, including non-Hodgkin's lymphomas, such as mantle cell lymphoma, with good response rates (16). However, many cancer patients treated with rapamycin analogues do not respond and this makes the use of *mTOR* siRNA an interesting alternative gene therapy approach, at least from the theoretical point of view.

In summary, we have shown that mTOR signaling is frequently activated in ALK+ ALCL and depends, in part, on activation of PI3K/AKT pathway. Inhibition of the mTOR pathway interferes with essential proliferation and survival pathways in ALK+ ALCL and might form the basis for a novel therapeutic strategy.

Acknowledgments

Received 8/30/2005; revised 4/4/2006; accepted 4/20/2006.

Grant support: The University of Texas M.D. Anderson Cancer Center institutional research grant (G.Z. Rassidakis).

The costs of publication of this article were defrayed in part by the payment of page charges. This article must therefore be hereby marked *advertisement* in accordance with 18 U.S.C. Section 1734 solely to indicate this fact.

We thank Dr. K. Walsh for providing us with the myrAkt adenoviral vector.

References

1. Delsol G, Ralfkiaer E, Stein H, Wright D, Jaffe ES. Anaplastic large cell lymphoma. In: Jaffe ES, Harris NL, Stein H, Vardiman JW, editors. World Health Organization classification of tumours. Pathology and genetics of tumors of haematopoietic and lymphoid tissues. Lyon (France): IARC Press; 2001. p.230–5.
2. Duyster J, Bai RY, Morris SW. Translocations involving anaplastic lymphoma kinase (ALK). Oncogene 2001;20:5623–37.
3. Morris SW, Kirstein MN, Valentine MB, et al. Fusion of a kinase gene, ALK, to a nucleolar protein gene, NPM, in non-Hodgkin's lymphoma. Science 1994;263:1281–4.
4. Bai RY, Ouyang T, Miething C, Morris SW, Peschel C, Duyster J. Nucleophosmin-anaplastic lymphoma kinase associated with anaplastic large-cell lymphoma activates the phosphatidylinositol 3-kinase/Akt antiapoptotic signaling pathway. Blood 2000;96:4319–27.
5. Slupianek A, Nieborowska-Skorska M, Hoser G, et al. Role of phosphatidylinositol 3-kinase-Akt pathway in nucleophosmin/anaplastic lymphoma kinase-mediated lymphomagenesis. Cancer Res 2001;61:2194–9.
6. Peng XD, Xu PZ, Chen ML, et al. Dwarfism, impaired skin development, skeletal muscle atrophy, delayed bone development, and impeded adipogenesis in mice lacking Akt1 and Akt2. Genes Dev 2003;17:1352–65.
7. Hara K, Maruki Y, Long X, et al. Raptor, a binding partner of target of rapamycin (TOR), mediates TOR action. Cell 2002;110:177–89.
8. Loewith R, Jacinto E, Wullschleger S, et al. Two TOR complexes, only one of which is rapamycin sensitive, have distinct roles in cell growth control. Mol Cell 2002;10:457–68.
9. Pullen N, Thomas G. The modular phosphorylation and activation of p70s6k. FEBS Lett 1997;410:78–82.
10. Burnett PE, Barrow RK, Cohen NA, Snyder SH, Sabatini DM. RAFT1 phosphorylation of the translational regulators p70 S6 kinase and 4E-BP1. Proc Natl Acad Sci U S A 1998;95:1432–7.
11. Schmelzle T, Hall MN. TOR, a central controller of cell growth. Cell 2000;103:253–62.
12. Sonenberg N, Gingras AC. The mRNA 5′ cap-binding protein eIF4E and control of cell growth. Curr Opin Cell Biol 1998;10:268–75.
13. Sarbassov DD, Guertin DA, Ali SM, Sabatini DM. Phosphorylation and regulation of Akt/PKB by the rictor-mTOR complex. Science 2005;307:1098–101.
14. Douros J, Suffness M. New antitumor substances of natural origin. Cancer Treat Rev 1981;8:63–87.
15. Eng CP, Sehgal SN, Vezina C. Activity of rapamycin (AY-22,989) against transplanted tumors. J Antibiot (Tokyo) 1984;37:1231–7.
16. Witzig TE, Geyer SM, Ghobrial I, et al. Phase II trial of single-agent temsirolimus (CCI-779) for relapsed mantle cell lymphoma. J Clin Oncol 2005;23:5347–56.
17. Brown VI, Fang J, Alcorn K, et al. Rapamycin is active against B-precursor leukemia *in vitro* and *in vivo*, an effect that is modulated by IL-7-mediated signaling. Proc Natl Acad Sci U S A 2003;100:15113–8.
18. Kim DH, Sarbassov DD, Ali SM, et al. mTOR interacts with raptor to form a nutrient-sensitive complex that signals to the cell growth machinery. Cell 2002;110:163–75.
19. Oshiro N, Yoshino K, Hidayat S, et al. Dissociation of raptor from mTOR is a mechanism of rapamycin-induced inhibition of mTOR function. Genes Cells 2004;9:359–66.
20. Rassidakis GZ, Feretzaki M, Atwell C, et al. Inhibition of Akt increases $p27^{Kip1}$ levels and induces cell cycle arrest in anaplastic large cell lymphoma. Blood 2005;105:827–9.
21. Rassidakis GZ, Claret FX, Lai R, et al. Expression of p27(Kip1) and c-Jun activation binding protein 1 are inversely correlated in systemic anaplastic large cell lymphoma. Clin Cancer Res 2003;9:1121–8.
22. Rassidakis GZ, Jones D, Thomaides A, et al. Apoptotic

rate in peripheral T-cell lymphomas. A study using a tissue microarray with validation on full tissue sections. Am J Clin Pathol 2002;118:328–34.
23. Fujio Y, Guo K, Mano T, Mitsuuchi Y, Testa JR, Walsh K. Cell cycle withdrawal promotes myogenic induction of Akt, a positive modulator of myocyte survival. Mol Cell Biol 1999;19:5073–82.
24. Brown EJ, Beal PA, Keith CT, Chen J, Shin TB, Schreiber SL. Control of p70S6 kinase by kinase activity of FRAP *in vivo*. Nature 1995;377:441–6.
25. Bjornsti MA, Houghton PJ. The TOR pathway: a target for cancer therapy. Nat Rev Cancer 2004;4:335–48.
26. Vivanco I, Sawyers CL. The phosphatidylinositol 3-kinase AKT pathway in human cancer. Nat Rev Cancer 2002;2:489–501.
27. Sekulic A, Hudson CC, Homme JL, et al. A direct linkage between the phosphoinositide 3-kinase-AKT signaling pathway and the mammalian target of rapamycin in mitogen-stimulated and transformed cells. Cancer Res 2000;60:3504–13.
28. Reynolds TH, Bodine SC, Lawrence JC, Jr. Control of Ser^{2448} phosphorylation in the mammalian target of rapamycin by insulin and skeletal muscle load. J Biol Chem 2002;277:17657–62.
29. Harris TE, Lawrence JC, Jr. TOR signaling. Sci STKE 2003;2003:re15.
30. Pyronnet S, Sonenberg N. Cell-cycle-dependent translational control. Curr Opin Genet Dev 2001;11:13–8.
31. Hammond ML, Bowman LH. Insulin stimulates the translation of ribosomal proteins and the transcription of rDNA in mouse myoblasts. J Biol Chem 1988;263:17785–91.
32. Harada H, Andersen JS, Mann M, Terada N, Korsmeyer SJ. p70S6 kinase signals cell survival as well as growth, inactivating the pro-apoptotic molecule BAD. Proc Natl Acad Sci U S A 2001;98:9666–70.
33. Shima H, Pende M, Chen Y, Fumagalli S, Thomas G, Kozma SC. Disruption of the p70(s6k)/p85(s6k) gene reveals a small mouse phenotype and a new functional S6 kinase. EMBO J 1998;17:6649–59.
34. Meyuhas O. Synthesis of the translational apparatus is regulated at the translational level. Eur J Biochem 2000;267:6321–30.
35. Sahin F, Kannangai R, Adegbola O, Wang J, Su G, Torbenson M. mTOR and p70 S6 kinase expression in primary liver neoplasms. Clin Cancer Res 2004;10:8421–5.
36. Kim JE, Chen J. Cytoplasmic-nuclear shuttling of FKBP12-rapamycin-associated protein is involved in rapamycin-sensitive signaling and translation initiation. Proc Natl Acad Sci U S A 2000;97:14340–5.
37. Wendel HG, De Stanchina E, Fridman JS, et al. Survival signalling by Akt and eIF4E in oncogenesis and cancer therapy. Nature 2004;428:332–7.
38. Lazaris-Karatzas A, Smith MR, Frederickson RM, et al. Ras mediates translation initiation factor 4E-induced malignant transformation. Genes Dev 1992;6:1631–42.
39. Wang S, Rosenwald IB, Hutzler MJ, et al. Expression of the eukaryotic translation initiation factors 4E and 2α in non-Hodgkin's lymphomas. Am J Pathol 1999;155:247–55.
40. Jones RM, Branda J, Johnston KA, et al. An essential E box in the promoter of the gene encoding the mRNA cap-binding protein (eukaryotic initiation factor 4E) is a target for activation by c-myc. Mol Cell Biol 1996;16:4754–64.
41. Schalm SS, Blenis J. Identification of a conserved motif required for mTOR signaling. Curr Biol 2002;12:632–9.
42. Schalm SS, Fingar DC, Sabatini DM, Blenis J. TOS motif-mediated raptor binding regulates 4E-BP1 multisite phosphorylation and function. Curr Biol 2003;13:797–806.
43. Chiang GG, Abraham RT. Phosphorylation of mammalian target of rapamycin (mTOR) at Ser-2448 is mediated by p70S6 kinase. J Biol Chem 2005;280:25485–90.
44. Holz MK, Blenis J. Identification of S6K1 as a novel mTOR-phosphorylating kinase. J Biol Chem 2005;280:26089–93.
45. Gera JF, Mellinghoff IK, Shi Y, et al. AKT activity determines sensitivity to mammalian target of rapamycin (mTOR) inhibitors by regulating cyclin D1 and c-myc expression. J Biol Chem 2004;279:2737–46.
46. Huang S, Liu LN, Hosoi H, Dilling MB, Shikata T, Houghton PJ. p53/p21(CIP1) cooperate in enforcing rapamycin-induced G(1) arrest and determine the cellular response to rapamycin. Cancer Res 2001;61:3373–81.